Temporal characteristics of functional connectome reconfigurations are heritable and related to cognition.

Suhnyoung Jun[1,2], Thomas H. Alderson[1], Andre Altmann[3], Sepideh Sadaghiani[1,2,4]*

[1] Beckman Institute for Advanced Science and Technology, University of Illinois at Urbana-Champaign, Urbana, Illinois, 618201
[2] Psychology Department, University of Illinois at Urbana-Champaign, Urbana, Illinois 61801
[3] Centre for Medical Image Computing (CMIC), Department of Medical Physics, University College London, London, UK
[4] Neuroscience Program, University of Illinois at Urbana-Champaign, Urbana, Illinois 61801

***Correspondence**: Sepideh Sadaghiani
Email: sepideh@illinois.edu

Author Contributions: SJ and SS designed research; SJ performed research; SJ analyzed data; SJ and SS wrote the paper; and SS, THA and AA contributed analytic expertise, theoretical guidance, paper revisions, and informed interpretation of the results.

Competing Interest Statement: The authors declare no competing interest.

Keywords: dynamic functional connectivity; heritability; variance component modeling; twin study, hidden Markov modelling.

This PDF file includes:

Main Text
Figures 1 to 4
Table 1

Abstract

The brain's functional connectivity architecture is dynamic, constantly reconfiguring in an individual-specific manner and contributing to inter-individual variability in cognitive abilities. However, to what extent genetic effects shape the dynamic reconfigurations of the functional connectome is largely unknown. This paper assesses whether dynamic connectome features are heritable, quantifies their heritability, and explores their association with cognitive phenotypes. We identified discrete connectome states from resting-state fMRI data (n = 1003 including twins and non-twin siblings) and obtained multivariate features, each describing temporal or spatial characteristics of connectome dynamics. We found strong evidence that the temporal features, particularly fractional occupancy (FO) and transition probability (TP), were heritable. Importantly, a substantial proportion of phenotypic variance of these features (specifically, 35% of FO and 41% of TP) was explained by genetic effects. The effect was stable after adjusting for head motion, independent of global signal regression and the chosen number of states, and absent in surrogate data. Contrarily, the data did not provide robust support for the heritability of the spatial features. Genetic effects may therefore primarily contribute to how the connectome *transitions* across states, rather than the precise way in which the states are spatially instantiated. Notably, we showed that the temporal phenotypes also capture variability in cognitive performance. In summary, the genetic makeup impacts the temporal reconfiguration of the functional connectome, and such dynamic features may act as endophenotypes for cognitive abilities. We propose that connectome dynamics offer considerable potential as a theoretical and practical framework for linking genetics to behavior.

Significance Statement

The spatial organization of human brain functional connectivity, or the connectome, is highly dynamic. While such time-varying dynamics explain differences in cognition across individuals, it is unknown to what degree they are heritable. We provide evidence that genetic contributions to temporal features of connectome dynamics are substantial. Further, we establish a link between heritable connectome dynamics and heritable cognitive traits. Our results suggest that temporal connectome dynamics in the resting human brain constitute endophenotypes for cognitive abilities and may serve as candidates for biomarkers and inform the identification of functionally relevant genes and polymorphisms.

Introduction

Inter-individual variability in the time-averaged (static) functional connectivity architecture of the human brain is subject-specific and predictive of cognitive abilities (1–4). With the increasing availability of large-sample fMRI datasets, significant genetic contributions to this static large-scale connectome architecture have been established. Specifically, individual edge-wise connections and networks of the functional connectome have been identified as heritable (5, 6). Moreover, topological properties of the static connectome, such as the modular organization, have been shown to constitute heritable subject-specific traits linked to behavioral and cognitive characteristics (7, 8).

However, the static architecture captures only part of the functionally significant properties of the connectome. In fact, the functional connectome as measured by fMRI exhibits flexible reconfigurations over the course of seconds to minutes (9, 10). These reconfigurations can be described as changes in connectivity strength between specific sets of brain region-pairs, forming recurrent connectome states. Such functional connectome states hold great significance as their time-varying (dynamic) characteristics have been linked to behavior and cognition (11, 12).

Because some of the same behavioral and cognitive features linked to connectome dynamics are also heritable (13), the novel possibility that the behaviorally relevant connectome dynamics may themselves be heritable emerges. In light of this, we argue that future advances are contingent upon identifying those features of functional connectome dynamics that are heritable and linked to behavior. Therefore, in the following we focus on some of the key connectome feature previously identified as behaviorally relevant.

An often-reported observation is that dynamic changes in the *spatial* features of the connectome shape behavior. In particular, behavioral outcomes have been linked to variability of functional connectivity (FC) between the default-mode network (DMN) and top-down control regions (14, 15). Most notably, FC dynamics between the DMN and the frontoparietal network (FPN) have been linked to cognitive flexibility (16–18). Spatial connectome patterns can further be quantified as global topological properties of the connectome's graph. Modularity quantifies the balance between segregation (prioritizing processing within specialized networks) and integration (combining specialized information from various networks) (19). Modularity is the topological feature for which dynamics (20) are most commonly associated with various behaviors (14, 21–23).

Beyond these spatial attributes of connectome organization, specific *temporal* features of connectome dynamics have been shown to be behaviorally relevant (24). Specifically, the proportion of the total recording time spent in each connectome state (fractional occupancy, or FO) and the probability to transition between specific pairs of discrete states (transition probability, or TP) have been linked to behavior (11, 12). Moreover, the time spent in two "meta-states", identified

from hierarchical clustering of FO over fine-grained states, was found to be heritable (12). Temporal features characterizing connectome dynamics are of particular interest, as they define the *trajectory* of the connectome through state space rather than the states themselves. In fact, the matrix of TP values between all possible state-pairs fully characterizes connectome transitions.

Based on the preceding evidence, we chose to investigate two spatial features, FC between DMN and FPN ($FC_{DMN\text{-}FPN}$) and Modularity, and two temporal features, FO and TP between states. We sought to answer (i) whether spatial and topological features of discrete connectome states are heritable; (ii) whether temporal features associated with the spontaneous reorganization of these states are heritable; (iii) whether dynamic connectome features are inherited individually or collectively as multivariate traits; (iv) how much of the individual phenotypic differences can be accounted for by genetic influence; and (v) how inter-individual variability in heritable connectome dynamics contributes to differences in cognitive ability. To address these questions, we extracted discrete brain states from resting-state fMRI data acquired from the Human Connectome Project (25), including monozygotic and dizygotic twin pairs, non-twin sibling pairs, and pairs of unrelated individuals, estimated their dynamic features, fitted quantitative genetic models to the features, and quantified their association with cognition.

Results

Fig. 1 is a schematic representation of the overall approach and each subsection of the analysis.

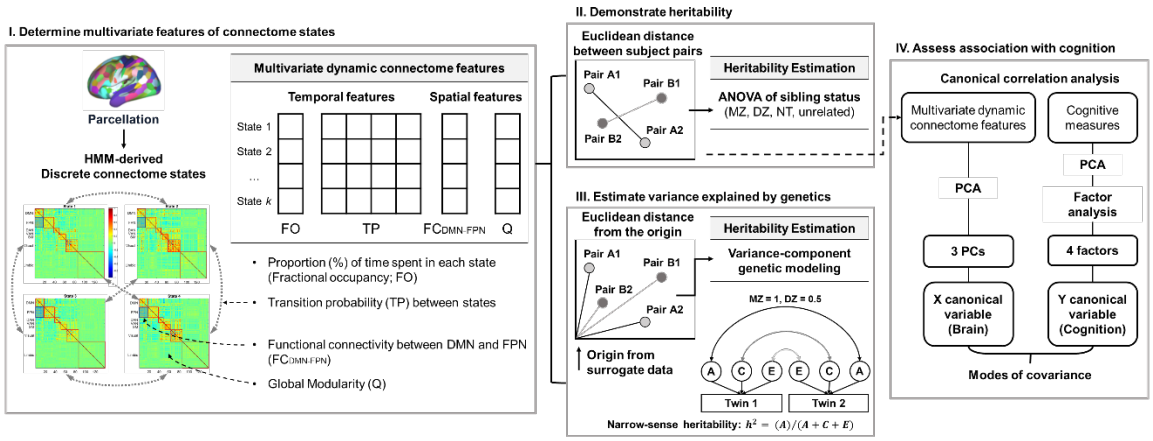

Fig. 1. An overview of the method pipeline. We used minimally preprocessed resting state BOLD timeseries from 139 group-ICA-derived regions covering cortical and subcortical areas of the cerebrum as provided by the Human Connectome Project. [Section I] We used a hidden Markov

model (HMM) to extract four discrete connectome states (or six states for replication). Four subject-level multivariate features describing the connectome dynamics were obtained. Multivariate temporal features were defined as the proportion of the recording time spent in each connectome state (fractional occupancy, or FO) and the probability matrix of transitioning between every pair of discrete states (transition probability, or TP). Multivariate spatial features included the functional connectivity between default mode and frontoparietal networks ($FC_{DMN\text{-}FPN}$) and global modularity (Q). All state-specific features (i.e., FO, $FC_{DMN\text{-}FPN}$, and Q) differed significantly across states. [Section II] We tested whether genetically related subjects displayed greater similarity in their multivariate features than genetically less related subjects. The similarity of each feature between a given pair of subjects was quantified as Euclidean distance. A one-way ANOVA was performed on the distance values of the factor sibling status with four levels including monozygotic twins (MZ; 120 pairs), dizygotic twins (DZ; same-sex 65 pairs), non-twin siblings (NT; 169 pairs), and pairs of unrelated individuals (88 pairs). [Section III] To estimate the heritability and quantify the genetic effects, we employed structural equation modeling (i.e., genetic variance component model). Phenotypic variance of a trait was partitioned into additive genetic (denoted A), common environmental (denoted C) and unique environmental components (denoted E), with narrow-sense heritability (h^2) quantified as the proportion of variance attributed to the genetic factor (A). Path A is dependent on the genetic similarity between twins. MZ twins are genetically identical (path denoted MZ = 1), whereas DZ twins based on the supposition of Mendelian inheritance share half of their genetic information (path denoted DZ = 0.5). Multivariate features were accommodated by computing the distance between the position of the feature and a null model-derived tangent point in multivariate space. [Section IV] Finally, canonical correlation analysis (CCA) was used to find modes of population covariation between multivariate dynamic connectome features and cognition. CCA analysis was performed on dimension-reduced data including three multivariate dynamic connectome feature principal components and four cognitive factors.

I. Discrete connectome states have distinct spatial and temporal profiles

We extracted four discrete connectome states, i.e., whole-brain recurrent connectivity patterns, in a data-driven fashion using hidden Markov modeling (HMM) (Fig. 2A) (26). Since HMMs require an *a priori* selection of the number of states (K), we chose two values of K within the range of prior HMM literature (K = 3 to 12 (12, 26–32)). We show that robust heritability effects are observable in both parameter regimes. We report outcomes for K = 4 in the following and provide replicated results for K = 6 in *SI Appendix*.

To assess whether the HMM-derived states possessed distinguishable network organization, a one-way ANOVA (factor state) of the connectome states' temporal and spatial

features of interest was conducted. Specifically, we tested the strength of FC between DMN and FPN ($FC_{DMN\text{-}FPN}$), the degree of global modular organization as measured by Newman's Modularity (33), and the proportion of time spent in each state, or Fractional Occupancy (FO).

Fig. 2B shows that the connectome states differed with respect to $FC_{DMN\text{-}FPN}$ ($F_{(3,\ 3976)}$ = 399.41 with p = 1.18e-217), Modularity ($F_{(3,\ 3717)}$ = 189.65 with p = 1.96e-114), and FO ($F_{(3,\ 3996)}$ = 105.00 with p = 1.98e-65). An exploratory whole-connectome comparison of connection-wise (edge-wise) FC strength further supported that FC differed across states beyond $FC_{DMN\text{-}FPN}$ in a spatially distributed set of connections (Fig. 2C; and *Fig. S5*). Regarding temporal characteristics, the distribution of FO over the states as well as the TP between states were not random (tested for the four- and six-state models against surrogate data, *SI Appendix, Fig. S10*). The present results indicate that the spontaneous connectivity time courses can be described as non-random sequences of four (or six) connectome states that differ from each other in terms of spatial organization, global topology, and proportion of occurrence.

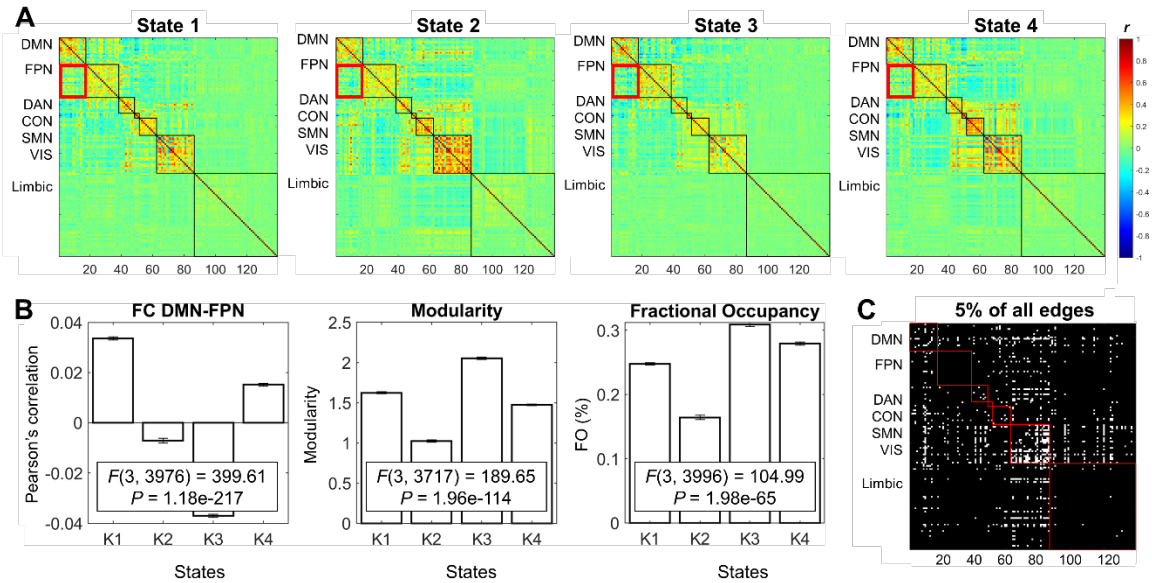

Fig. 2. HMM-inferred connectome states. (A) Group-level HMM-derived states corresponding to z-scored functional correlations of 139 cortical and subcortical regions. The rows and columns represent regions organized according to canonical ICN membership (34) including visual network (VIS), sensory-motor network (SMN), dorsal attention network (DAN), salience/cingulo-opercular network (CON), limbic network (Limbic), frontoparietal network (FPN), and default mode network (DMN). Red square indicates the functional connections between DMN and FPN ($FC_{DMN\text{-}FPN}$) corresponding to an *a priori* selected spatial feature. (B) Bar plots of the mean $FC_{DMN\text{-}FPN}$, Modularity,

and FO for each state (1003 subjects). *F* values are reported for one-way ANOVAs of the factor state for each variable. Strong differences across states are observed in all three measures. (C) A binary matrix showing a topological cluster of connections (edges) with significant FC difference across the four states. *F* values from an edge-wise ANOVA of FC strength were threshold at 5% edge density followed by network-based statistics (NBS) to control for multiple comparisons (35). Significant connections are widely distributed across networks, prominently including the DMN and VIS. For details, see *Fig. S5* and *SI Appendix*– *Exploring heritability with network-based statistics*.

II. Multivariate temporal features of the dynamic connectome are heritable.

To circumvent the statistical limitations imposed through multiple comparisons, the heritability analysis was limited to a selection of hypothesis-driven phenotypes. State-specific features including $FC_{DMN\text{-}FPN}$, Modularity, and FO, and TPs between states were interrogated for heritability by treating the $1 \times K$ vectors of $FC_{DMN\text{-}FPN}$, Modularity, FO, and $K \times K$ matrix of TP as *multivariate* features.

We tested the supposition that genetically related subjects had more similar multivariate features than genetically less related subjects. The similarity of each multivariate connectome feature between a given pair of subjects was quantified as Euclidean distance (**Materials and Methods** – Comparison of multivariate features). Distance values entered a one-way ANOVA of the factor sibling status with four levels, including monozygotic (MZ) twins, same-sex dizygotic (DZ) twins, non-twin (NT) siblings, and pairs of unrelated individuals. No subjects overlapped between groups.

Fig. 3A indicates which temporal features of the connectome dynamics are heritable. Specifically, multivariate FO ($F_{(3, 438)} = 22.65$, $P = 1.19e\text{-}13$) and TP ($F_{(3, 438)} = 17.91$, $P = 5.57e\text{-}11$) phenotypes were more similar among MZ twins than DZ twins, followed by NT siblings and pairs of unrelated individuals. The effect of sibling status on multivariate dynamic connectome features was stable after adjusting for head motion parameters and independent of global signal regression (GSR) and the chosen number of states (see *SI Appendix* – *Independence of heritability from parameter choices*, *Fig. S2*). Further, no effect of sibling status was observed in surrogate data with preserved static covariance structure; FO ($F_{(3, 438)} = 1.30$, $p = .27$) and TP ($F_{(3, 438)} = 1.14$, $p = .33$).

Contrary to the temporal features, robust evidence for the heritability of multivariate spatial features was lacking. In particular, outcomes of equivalent ANOVAs for $FC_{DMN\text{-}FPN}$ ($F_{(3, 438)} = 3.40$, $P = 0.018$) and Modularity ($F_{(3, 438)} = 3.47$, $P = 0.016$) were small in effect size and dependent on the chosen number of states and global signal regression (*SI Appendix* – *Independence of heritability from parameter choices*, *Fig. S3*). This lack of heritability was confirmed by a subsequent variance-component genetic analysis (see section III.).

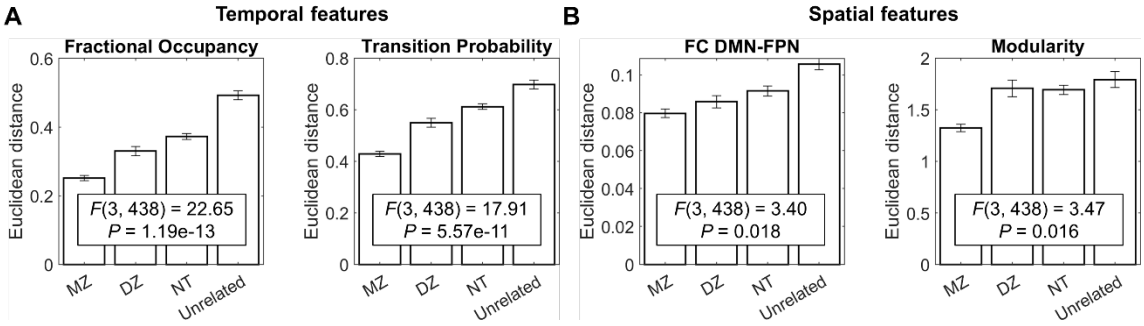

Fig. 3. Heritability of multivariate dynamic connectome features. Heritability was assessed by comparing the multivariate features across monozygotic twins (MZ; 120 pairs), dizygotic twins (DZ; 65 pairs), non-twin siblings (NT; 169 pairs), and pairs of unrelated individuals (88 pairs). *F* values are reported for one-way ANOVAs of the factor sibling status with four levels. A) Temporal connectome features, specifically the multivariate FO and TP phenotypes, were more similar among MZ twin pairs than DZ twins, followed by NT siblings and pairs of unrelated individuals. The influence of sibling status on multivariate dynamic connectome features was statistically significant and stable, irrespective of global signal regression (GSR) and the chosen number of states (see *Fig. S2*). B) Spatial connectome features, including $FC_{DMN\text{-}FPN}$ and Modularity, showed significant difference across sibling groups in the four-state model visualized here, but the statistical significance was not reproduced in the six-state model (see *Fig. S3*).

To ensure that the lack of a robust outcome for spatial attributes was not driven by a narrow feature selection, we further performed exploratory ANOVAs to assess the heritability of FC between DMN and the two other major top-down control networks (*SI Appendix – Exploring heritability of DMN connectivity to other networks*, *Fig. S4*), as well as a data-driven selection of edges (*SI Appendix – Exploring heritability with network-based statistics*, *Fig. S5*). Again, ANOVA outcomes were either dependent on the number of states and GSR or inconsistent with expectations. For example, DZ twins showed less similarity than NT siblings, suggesting that these spatial features may not be heritable. Potential reasons for such inconsistencies are discussed in the *SI Appendix*.

Importantly, the *individual* components of multivariate features were not heritable (*Fig. S7*); none of the state-wise dynamic connectome phenotypes differed by sibling status, even though they showed clear differences across connectome states (See *Fig. S6* for the main effect of connectome states, in line with results of Fig. 2B). Our findings demonstrate that temporal features

of the dynamic connectome are heritable, only when considered as multivariate patterns, rather than as individual state-specific components.

III. Heritability accounts for differences in multivariate dynamic connectome features across individuals.

We employed structural equation modeling (36) to estimate the extent to which inter-individual differences in a phenotype are driven by genetic or environmental factors. The classical genetic variance component model quantifies the contribution of genetic factors to univariate phenotypes. However, our above-described ANOVAs suggest that temporal characteristics of connectome dynamics are inherited as ***multivariate*** phenotypes (Fig. 3A) rather than individual components (*Fig. S7*). The variance component model of univariate features was therefore adjusted to accommodate multivariate phenotypes. This was accomplished by defining the position of the feature in multivariate space (cf. Fig. 1). For completeness, an alternative approach (37) for multivariate features, which however does not account for collinearities among the univariate components, is included in *SI Appendix – Alternative multivariate genetic variance component model* and *Table S2*.

The ACE model explained a substantial portion of variance of multivariate temporal dynamic connectome features in terms of genetic effect (Table 1). The additive genetic effect (A) of FO was estimated as .35, corresponding to a narrow-sense heritability of h^2 = .35 (i.e., accounting for 35% of the total phenotypic variance). The additive genetic effect of TP was estimated as .41, corresponding to a narrow-sense heritability of h^2 =.41, again accounting for a substantial proportion of inter-individual variance in this measure. Note that the impact of common environment (C) was estimated as zero for both FO and TP. For both features, the fitness of the nested models was not significantly better than the full ACE model. These outcomes indicate that genetics contribute substantially to the temporal features of connectome dynamics.

Contrary to the temporal features, the variance component modeling of the spatial features, $FC_{DMN\text{-}FPN}$ and Modularity, did not support a genetic effect. The h^2 of $FC_{DMN\text{-}FPN}$ was .21, but with a wide 95% confidence interval crossing zero ([-0.30, 0.72]). No heritability was found for Modularity (h^2=0). This outcome confirms the lack of robust heritability effect observed from the ANOVA (Fig. 3 and *Fig. S3*) for $FC_{DMN\text{-}FPN}$ and Modularity.

IV. Temporal phenotypes of the dynamic connectome are associated with cognition

Finally, canonical correlation analysis (CCA) was used to relate the cognitive measures to temporal phenotypes of the dynamic connectome. The CCA, performed on three principal components of dynamic connectome phenotypes and four factors of cognitive measures obtained

from all subjects with complete cognitive measures (n = 997), revealed three modes of covariation (Fig. 4A). Two modes were highly significant (against 10,000 permutations, $p < 10^{-4}$ (Fig. 4B-C)) and robust after correcting for frame-wise displacement (FD). To reveal the contribution of each cognitive factor to each mode, the modes and the cognitive factors were post-hoc correlated. The first mode with the highest significance was defined by negative weights for the "Language" (r = -.20) and "Memory" (r = -.18) factors, followed by "Impulsivity" (r = -.14) and "Cognitive control" (r = -.12; Fig. 4D). The second mode was defined by a positive weight for "Cognitive control" (r = .07; Fig. 4E). Together, these findings suggest that temporal phenotypes of the dynamic connectome are related to cognitive performance.

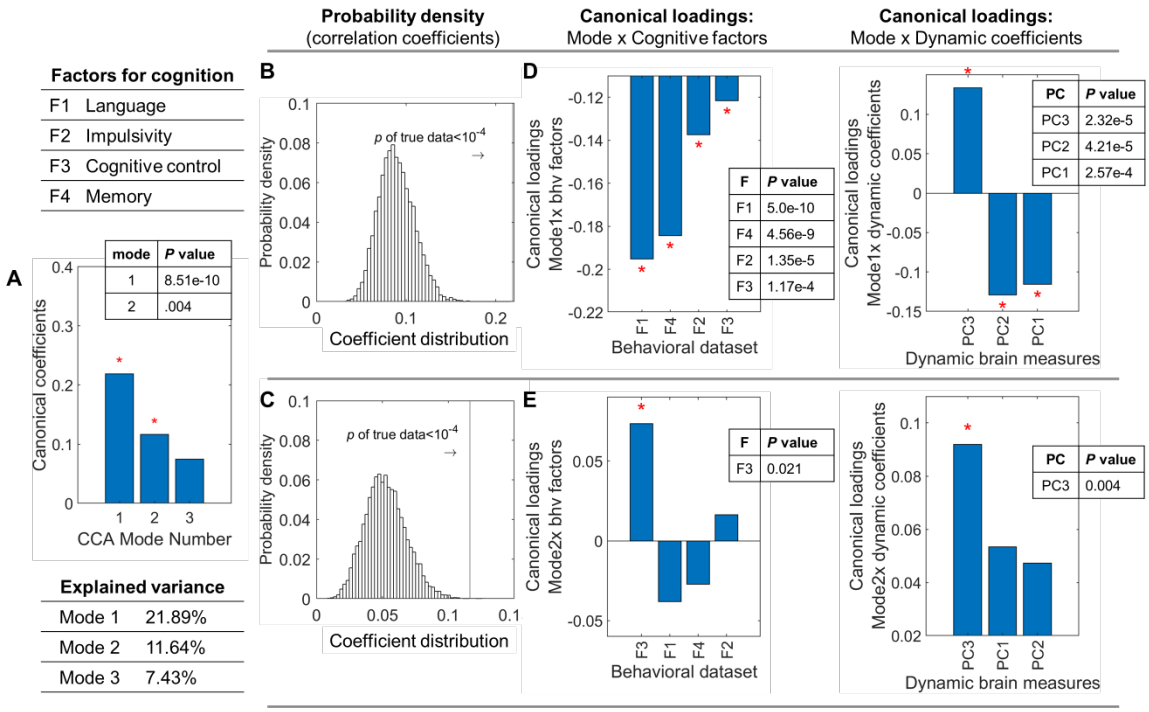

Fig. 4. Dynamic connectome features are related to cognition. (A) Canonical variable X was defined as three principal components, explaining about 88.27% of the total variance in the temporal phenotypes of the dynamic connectome. Canonical variable Y was defined as four factors, explaining about 54.86 % of the total variance in the cognitive measures. Canonical correlation analysis (CCA) revealed two significant modes of covariation between these two canonical variables. (B-C) A null distribution of canonical variate pair correlation values was constructed using 10,000 random permutations of the rows of X relative to the rows of Y (respecting the within-participant structure of the data) (38). Compared to the null distribution, each mode of covariation

in the true data was highly significant ($p < 10^{-4}$). (D-E) Post-hoc analysis showed the contribution of the respective variable to each mode. Left panels show the contribution of cognitive factor loadings to each mode, and right panels show the contribution of PC coefficients of connectome dynamics phenotypes to each mode (in ascending order of *p*-value). $P < .05$ are marked with an asterisk. F, factor loading; PC, principal component.

Discussion

The present interest in time-varying dynamics of the functional connectome is rooted in its potential to transform our understanding of fundamental cognitive processing within and across individuals. However, the growing literature on heritability of connectome features has largely overlooked the connectome's inherently dynamic and multivariate character. Because characterization of dynamic connectome reconfigurations involves multiple states, we defined multivariate dynamic phenotypes that incorporate differential contributions from all states simultaneously. Applying this novel multivariate approach to both temporal and spatial phenotypes, we showed that multivariate dynamic features offer robust evidence of heritability (Fig. 2 and *Fig. S2*), contrasting scalar features (*Fig. S7*). Moreover, the quantitative genetic modeling provided converging evidence for a robust genetic effect and the first quantitative heritability estimates of dynamic connectome features (Table 1). Overall, our findings provide strong evidence supporting the substantial genetic influence on temporal characteristics of connectome dynamics, which explain individual differences in cognitive abilities.

Previous studies based on the classical twin designs have found considerable genetic effects on multiple structural and *static* (i.e., time-averaged) functional connectome features of the human brain. Heritable features of the structural connectome include size (h^2 = 23-60%) and topography (h^2 = 12-19%) of ICNs (39), and average regional controllability as derived from network control theory (h^2 = 13-64%) (40). Regarding the functional connectome, heritability has been established for static FC within canonical neurocognitive ICNs in several studies (h^2 = 13–36% (41); h^2 = 45-80% (5); (h^2 = 9-28% (42)). Further, genetic effects have been reported for topological properties of the static functional connectome, such as global efficiency (h^2 = 52-62%), mean clustering coefficient (h^2 = 47-59%), small-worldness (h^2 = 51-59%), and modularity (h^2 = 38-59%) (8). Of note, all these structural and functional studies estimated heritability separately for each univariate connectome feature, of which the present multivariate approach represents a significant departure.

Beyond the above-described studies on structural and static functional connectomes, heritability and quantitative estimation of the genetic impact have been largely unknown for connectome dynamics. A single study has demonstrated heritability of the ratio of time spent across

two “meta-states”, defined from hierarchical clustering of FO over a 12-state model (12). This finding establishes the existence of a heritable temporal hierarchy of connectome dynamics. However, this study employed a univariate approach, and the multivariate features of the underlying states were not represented in the heritability assessment. Further, heritability of spatial characteristics of the dynamic states were not studied. Another important, open question is the magnitude of heritability, i.e., % variance of the dynamic features explained by genetic effects.

In this study, we established heritability of multivariate dynamic connectome phenotypes and quantified this influence using structural equation modeling (36). Importantly, we found that heritability of temporal characteristics of state transitions was under substantial genetic control. Specifically, the additive genetic effect on temporal phenotypes of the dynamic connectome was of high magnitude (h^2 of 35% and of 41% for FO and TP, respectively). This strong heritability is in the range reported above for structural and static FC investigations.

Interestingly, for both FO and TP the effect of common environment was estimated to be zero. To estimate the C factor, twin studies assume that environmental influences are common between MZ and DZ twins, and that the greater phenotypic similarity of MZs must therefore be due to their greater genetic similarity. However, both intrauterine and postnatal environments can differ as a function of zygosity (43). Therefore, the impact of common environment cannot be estimated with precision. Nonetheless, our estimated values suggest that the common environment is unlikely to have a sizable influence on these phenotypes.

Importantly, our findings suggest that differences in cognitive abilities are explained by heritable dynamic features. Multiple structural (40) and static functional connectome features (42, 44, 45) have shown their association with cognition. However, the link between functional connectome dynamics and cognitive measures is less well established (11, 12). Our study shows an association between multivariate temporal dynamic connectome phenotypes and cognitive measures and supports previous work suggesting potential genetic overlap between connectome dynamics and cognition (11, 12). Crucially, the cognitive measures that we investigated in our study are themselves known to be heritable in the HCP cohort (13). This may suggest that the dynamic connectome features identified in our study are potential endophenotypes for cognitive abilities.

In contrast to the temporal features, we found that heritability of spatial features of the dynamic connectome states was not robustly supported. Beyond the hypothesis-driven spatial features ($FC_{DMN\text{-}DAN}$ and Modularity) we tested for the heritability of additional features (i.e., $FC_{DMN\text{-}DAN}$, $FC_{DMN\text{-}CON}$, and data-driven clusters of connections) using ANOVAs and structural equation modelling; none were consistently significant across methodological choices (See *SI Appendix* – *Exploring heritability of DMN connectivity to other networks* and *Exploring heritability with network-based statistics*). In principle, this null result may be driven by limited signal-to-noise ratio, limited

statistical power, or other factors. However, the robust statistical power of temporal features combined with convergence of outcomes from the ANOVA and component modeling, suggests a genuine lack of effects for spatial features. We cautiously interpret our data to suggest that genetic effects primarily contribute to how the connectome *transitions* across different states, rather than the precise way in which the states are spatially instantiated in individuals.

Our study is subject to several limitations and methodological considerations. The available sample size is relatively small for a heritability study. Despite this limitation, the confidence intervals indicate that the sample size was sufficient to establish the genetic effect on FO and TP with high confidence. Another consideration is that our adaptation of genetic component modeling for multivariate features motivates a careful setting of the tangent point to avoid bias. We confirmed that the tangent point of the genetic model was chosen properly by demonstrating convergence of heritability estimates from the genetics model and the ANOVA approach (which is independent of the tangent point).

In conclusion, our multivariate approach provides converging evidence for a robust genetic effect on transitions between whole-brain connectome states and the proportion of time spent in each state. Our findings further indicate that the instantiation of subject-specific spatial layout of states is not heritable. Moreover, by establishing the association between heritable dynamic connectome features and heritable cognitive traits, the present study identifies TP and FO in the resting human brain as potential endophenotypes for cognitive abilities. As such, these features may translate to efficient connectome-based biomarkers and form the basis of targeted treatment across various cognitive domains.

Materials and Methods

Neuroimaging and Behavior Dataset

We used the Washington University-University of Minnesota (WU-Minn) consortium of the Human Connectome Project (HCP) S1200 release (46). Participants were recruited, and informed consent was acquired by the WU-Minn HCP consortium according to procedures approved by the Washington University IRB (47). For details of the HCP data collection protocol and cognitive measures, see (25, 46) and (48), respectively.

The analyses used all 1003 healthy adult subjects (aged 22-37 y, 534 females) with four complete resting-state fMRI runs (4800 total timepoints). The subjects include 120 monozygotic (MZ) twin pairs, 65 same-sex dizygotic (DZ) twin pairs, 169 non-twin (NT) sibling pairs, and 88 pairs of randomly matched unrelated individuals. Note that all pairs are uniquely defined so that none of the subjects overlap between groups. All 1003 subjects entered HMM estimation of discrete connectome states, while 884 subjects entered heritability analysis so as to avoid dependencies

across members of families with > 2 subjects. We included all 14 cognitive measures, which are summary scores for either a cognitive task or a questionnaire, under the cognition domain provided by the HCP (see S1 Table for more detailed description for each variable, and Fig. 1A for their phenotypic correlation structure). The measures were z-score normalized to zero mean and unit variance. Of 1003 subjects, 997 subjects had complete data for the 14 cognitive variables measuring cognitive performance and entered canonical correlation analysis (CCA).

Neuroimaging Data Preprocessing

All imaging data were acquired on a customized Siemens 3 T Skyra at Washington University in St. Louis using a multi-band sequence. Each 15-minute resting-state fMRI run was minimally preprocessed (47) using tools from FSL (49) and Freesurfer (50), and had artifacts removed using ICA+FIX (51, 52). Preprocessing following the pipeline of Smith et al. (25, 53). Inter-subject registration of cerebral cortex was carried out using areal-feature-based alignment and the Multimodal Surface Matching algorithm ('MSMAll') (54, 55). For group-PCA, each dataset was temporally demeaned and variance normalized (56). The data with the global signal removed (referred to as 'non-GSR data') was used for the main analysis. HCP provides averaged BOLD time-series for regions of group-ICA-based parcellations. We used the 300-independent component (IC) model, which better separates the individual regions of the intrinsic connectivity network (ICN) than the lower-order models. Of the 300 ICs, we retained 139 ICs corresponding to the regions of the cerebrum, excluding the cerebellum and brainstem. These regions were labeled according to the 7 canonical ICNs of the Yeo atlas (34) (*SI Appendix- Parcellations, Fig. S1*).

Hidden Markov modeling

We applied a hidden Markov model (HMM) to the minimally preprocessed region-wise BOLD time-series, resulting in *K* discrete states of whole-brain connectivity, each associated with state-specific time-course. The HMM assumes that time series data can be described using a finite sequence of a hidden number of states. Each state and its associated time series comprise a unique connectivity pattern that temporally re-occurs over time. Using the HMM-MAR (multivariate autoregressive) toolbox (26), states were inferred from region-wise BOLD time-series temporally concatenated across all subjects. Whereas the states are estimated at the group-level, each individual has a subject-specific state time course, indicating when a given state is active. For a given K, the best fitting model corresponding to the one with the lowest free energy was selected across five runs (26, 30, 32).

HMMs require an a priori selection of the number of states, *K*. Generally, the objective is not to establish a 'correct' number of states but to strike a balance between model complexity and

model fit and to identify a number that describes the dataset at a useful granularity (30). Prior HMM literature has used *K* ranging from 3 to 12 brain states (12, 26–32). We chose a similar parameter regime, between 4 and 6, reasoning that robust heritability effects would be evident in both. Note that our choice of *K* is in agreement with clustering methods which identify *K*s between 5 and 7 as optimal (24, 57–59).

Comparison of multivariate features

For each subject and HMM-derived state, we calculated FO (the cumulative total time spent in a given state), $FC_{DMN\text{-}FPN}$ (the mean connectivity across all regions of DMN with those of FPN), and Newman's Modularity (quantifying the level of segregation of each connectome state into modules (33), which are configured to use canonical ICNs (34) as the modular partition (Brain Connectivity Toolbox (60)). Further, for each subject, we estimated the transition probabilities across all state-pairs (TP matrix).

All features were multivariate in terms of *K*, the chosen number of discrete connectome states. These included FO ($1 \times K$), TP matrix ($K \times K$), $FC_{DMN\text{-}FPN}$ ($1 \times K$), and Modularity ($1 \times K$). To determine whether each feature was heritable as a multivariate phenotype, we estimated their similarity based on the Euclidean distance between subject pairs (61). Crucially, the positional relationship between elements in each multivariate variable was preserved. The genetic influence on the Euclidean distance was tested using an ANOVA of the factor sibling status with four levels (i.e., MZ twins, DZ twins, NT siblings, and pairs of unrelated individuals).

Additionally, we examined whether heritability of features was driven by multivariate patterns or by individual components. Specifically, we estimated the similarity of the FO, $FC_{DMN\text{-}FPN}$ and Modularity values of each state as the difference across subject pairs. Likewise, TP values of each state pair. Distance values were entered into a two-way ANOVA examining the effect of sibling status and connectome state.

Null model

Fifty simulated state time courses of the same length as the original empirical state time courses were generated using the *simhmmmar* function provided by HMM-MAR toolbox (26). Note that fifty is a robust number compared to previous work (e.g., Vidaurre et al. (12) applied four simulations). Surrogate data preserve the static covariance structure of the original data but destroy the precise temporal ordering of states. An HMM inference with $K = 4$ and $K = 6$, respectively, was run on each surrogate dataset and the dynamic connectome features (FO, TP, etc.) at the group- and subject-level were recomputed. The non-random distribution of features over states observed in the original dataset was absent in the surrogate dataset (*Fig. S10)*.

Quantification of heritability

The ACE genetic structural equation model compares the variance-covariance matrices between MZ and DZ twins. The approach assumes that MZ twins have identical genomes, whereas DZ twins share, on average, half of their genetic information. Assuming that environmental factors influence both types of twins to equally, the variance of a given phenotype can be partitioned into three latent components: additive genetic variance (A), resulting from additive effects of alleles at each contributing locus; shared environmental variance (C), resulting from common environmental effects for both members of a twin pair; and unique environmental variance (E), resulting from non-shared environmental (62). Nested models, specifically AE and CE, were fitted by dropping C or A, respectively. Statistical significance of nested models was assessed by a likelihood ratio test and the fitness of models was tested using the Akaike's Information Criterion (AIC) (63).

Variance component modeling was conducted using *twinlm* in the R package *mets* (http://cran.r-project.org/web/packages/mets/index.html), adjusting for age, sex, and FD (64). As the variance component model finds the relationship between twin pairs, the model requires each subject to have a singular value for each variable. Therefore, the subject-wise phenotypes were obtained by first finding a suitable Euclidean space for a given multivariate feature by taking the mean value of that feature from 50 surrogate datasets (See methods section on *null model*) as the tangent point. For each subject and feature, Euclidean distance from this tangent point was obtained for variance component modeling.

Canonical correlation analysis

Canonical correlation analysis (CCA) finds maximum correlations (or modes of population covariation) between multidimensional data (65), ameliorating the need to conduct all potential correlations and correct for multiple comparisons. As previously applied to the static connectome, we used CCA to relate cognitive measures to phenotypes of the dynamic connectome (11, 12, 38). We trained CCA on dimensionally reduced multivariate variables, including three dynamic connectome principal components and four cognitive factors. The contribution of each factor to the given mode was evaluated with post-hoc correlations between the modes and the cognitive factors. We further assessed the statistical significance of the discovered modes of covariation through 10,000 permutations. See *SI Appendix* – *canonical correlation analysis* for details.

Acknowledgments

Data were provided by the Human Connectome Project, WU-Minn Consortium (Principal Investigators: David Van Essen and Kamil Ugurbil; 1U54MH091657) funded by the 16 NIH Institutes and Centers that support the NIH Blueprint for Neuroscience Research; and by the McDonnell Center for Systems Neuroscience at Washington University. We would like to thank Jaime Derringer for her insight and interpretation of quantitative genetic modeling results. AA holds an MRC eMedLab Medical Bioinformatics Career Development Fellowship. This work was partly supported by the Medical Research Council (grant number MR/L016311/1). This work was supported by the National Institute for Mental Health (1R01MH116226 to Sepideh Sadaghiani).

References

1. E. S. Finn, *et al.*, Functional connectome fingerprinting: Identifying individuals based on patterns of brain connectivity. *Nat Neurosci* **18**, 1664–1671 (2015).

2. M. Jalbrzikowski, *et al.*, Functional connectome fingerprinting accuracy in youths and adults is similar when examined on the same day and 1.5-years apart. *Hum Brain Mapp* (2020) https:/doi.org/10.1002/hbm.25118.

3. O. T. Ousdal, *et al.*, Longitudinal stability of the brain functional connectome is associated with episodic memory performance in aging. *Hum Brain Mapp* **41**, 697–709 (2020).

4. M. D. Rosenberg, *et al.*, A neuromarker of sustained attention from whole-brain functional connectivity. *Nature Neuroscience* **19**, 165–171 (2016).

5. T. Ge, A. J. Holmes, R. L. Buckner, J. W. Smoller, M. R. Sabuncu, Heritability analysis with repeat measurements and its application to resting-state functional connectivity. *Proc Natl Acad Sci U S A* **114**, 5521–5526 (2017).

6. A. E. Reineberg, A. S. Hatoum, J. K. Hewitt, M. T. Banich, N. P. Friedman, Genetic and Environmental Influence on the Human Functional Connectome. *Cereb. Cortex* **30**, 2099–2113 (2020).

7. W. Liu, N. Kohn, G. Fernández, Intersubject similarity of personality is associated with intersubject similarity of brain connectivity patterns. *Neuroimage* **186**, 56–69 (2019).

8. B. Sinclair, *et al.*, Heritability of the network architecture of intrinsic brain functional connectivity. *Neuroimage* **121**, 243–252 (2015).

9. D. S. Bassett, *et al.*, Dynamic reconfiguration of human brain networks during learning. *Proc. Natl. Acad. Sci. U.S.A.* **108**, 7641–7646 (2011).

10. J. M. Shine, *et al.*, Human cognition involves the dynamic integration of neural activity and neuromodulatory systems. *Nature Neuroscience* **22**, 289–296 (2019).

11. A. Eichenbaum, I. Pappas, D. Lurie, J. R. Cohen, M. D'Esposito, Differential contributions of static and time-varying functional connectivity to human behavior. *Network Neuroscience*, 1–21 (2020).

12. D. Vidaurre, S. M. Smith, M. W. Woolrich, Brain network dynamics are hierarchically organized in time. *Proc. Natl. Acad. Sci. U.S.A.* **114**, 12827–12832 (2017).

13. Y. Han, R. Adolphs, Estimating the heritability of psychological measures in the Human Connectome Project dataset. *PLoS ONE* **15**, e0235860 (2020).

14. S. Sadaghiani, J.-B. Poline, A. Kleinschmidt, M. D'Esposito, Ongoing dynamics in large-scale functional connectivity predict perception. *PNAS* **112**, 8463–8468 (2015).

15. G. J. Thompson, *et al.*, Short-time windows of correlation between large-scale functional brain networks predict vigilance intraindividually and interindividually. *Human Brain Mapping* **34**, 3280–3298 (2013).

16. L. Douw, D. G. Wakeman, N. Tanaka, H. Liu, S. M. Stufflebeam, State-dependent variability of dynamic functional connectivity between frontoparietal and default networks relates to cognitive flexibility. *Neuroscience* **339**, 12–21 (2016).

17. P. J. Hellyer, *et al.*, The control of global brain dynamics: opposing actions of frontoparietal control and default mode networks on attention. *J Neurosci* **34**, 451–461 (2014).

18. D. Vatansever, A. E. Manktelow, B. J. Sahakian, D. K. Menon, E. A. Stamatakis, Angular default mode network connectivity across working memory load. *Human Brain Mapping* **38**, 41–52 (2017).

19. J. M. Shine, R. A. Poldrack, Principles of dynamic network reconfiguration across diverse brain states. *NeuroImage* **180**, 396–405 (2018).

20. R. F. Betzel, M. Fukushima, Y. He, X.-N. Zuo, O. Sporns, Dynamic fluctuations coincide with periods of high and low modularity in resting-state functional brain networks. *Neuroimage* **127**, 287–297 (2016).

21. J. R. Cohen, M. D'Esposito, The Segregation and Integration of Distinct Brain Networks and Their Relationship to Cognition. *J. Neurosci.* **36**, 12083–12094 (2016).

22. K. Finc, *et al.*, Transition of the functional brain network related to increasing cognitive demands. *Hum. Brain Mapp.* **3**, e17 (2017).

23. J. M. Shine, *et al.*, The Dynamics of Functional Brain Networks: Integrated Network States during Cognitive Task Performance. *Neuron* **92**, 544–554 (2016).

24. J. S. Nomi, *et al.*, Chronnectomic patterns and neural flexibility underlie executive function. *NeuroImage* **147**, 861–871 (2017).

25. S. M. Smith, *et al.*, Resting-state fMRI in the Human Connectome Project. *Neuroimage* **80**, 144–168 (2013).

26. D. Vidaurre, *et al.*, Spectrally resolved fast transient brain states in electrophysiological data. *Neuroimage* **126**, 81–95 (2016).

27. A. P. Baker, *et al.*, Fast transient networks in spontaneous human brain activity. *eLife* **3** (2014).

28. R. Becker, *et al.*, Transient spectral events in resting state MEG predict individual task responses. *NeuroImage* **215**, 116818 (2020).

29. T. Karapanagiotidis, *et al.*, The psychological correlates of distinct neural states occurring during wakeful rest. *Sci Rep* **10**, 21121 (2020).

30. A. J. Quinn, *et al.*, Task-Evoked Dynamic Network Analysis Through Hidden Markov Modeling. *Front Neurosci* **12** (2018).

31. A. B. A. Stevner, *et al.*, Discovery of key whole-brain transitions and dynamics during human wakefulness and non-REM sleep. *Nature Communications* **10**, 1035 (2019).

32. D. Vidaurre, *et al.*, Discovering dynamic brain networks from big data in rest and task. *Neuroimage* **180**, 646–656 (2018).

33. M. E. J. Newman, Finding community structure in networks using the eigenvectors of matrices. *Phys. Rev. E* **74**, 036104 (2006).

34. B. T. T. Yeo, *et al.*, The organization of the human cerebral cortex estimated by intrinsic functional connectivity. *J. Neurophysiol.* **106**, 1125–1165 (2011).

35. A. Zalesky, A. Fornito, E. T. Bullmore, Network-based statistic: identifying differences in brain networks. *Neuroimage* **53**, 1197–1207 (2010).

36. D. S. Falconer, *Introduction to quantitative genetics.*, 3rd Ed. (Longman Group, 1990).

37. T. Ge, *et al.*, Multidimensional heritability analysis of neuroanatomical shape. *Nat Commun* **7**, 13291 (2016).

38. S. M. Smith, *et al.*, A positive-negative mode of population covariation links brain connectivity, demographics and behavior. *Nature Neuroscience* **18**, 1565–1567 (2015).

39. K. M. Anderson, *et al.*, Heritability of individualized cortical network topography. *PNAS* **118** (2021).

40. W. H. Lee, A. Rodrigue, D. C. Glahn, D. S. Bassett, S. Frangou, Heritability and Cognitive Relevance of Structural Brain Controllability. *Cereb. Cortex* **30**, 3044–3054 (2020).

41. B. M. Adhikari, *et al.*, Comparison of heritability estimates on resting state fMRI connectivity phenotypes using the ENIGMA analysis pipeline. *Hum Brain Mapp* **39**, 4893–4902 (2018).

42. M. L. Elliott, *et al.*, General functional connectivity: Shared features of resting-state and task fMRI drive reliable and heritable individual differences in functional brain networks. *Neuroimage* **189**, 516–532 (2019).

43. D. Conley, E. Rauscher, C. Dawes, P. K. E. Magnusson, M. L. Siegal, Heritability and the Equal Environments Assumption: Evidence from Multiple Samples of Misclassified Twins. *Behav Genet* **43**, 415–426 (2013).

44. M. W. Cole, *et al.*, Multi-task connectivity reveals flexible hubs for adaptive task control. *Nature Neuroscience* **16**, 1348–1355 (2013).

45. M. P. van den Heuvel, O. Sporns, Network hubs in the human brain. *Trends in Cognitive Sciences* **17**, 683–696 (2013).

46. D. C. Van Essen, *et al.*, The WU-Minn Human Connectome Project: An Overview. *Neuroimage* **80**, 62–79 (2013).

47. M. F. Glasser, *et al.*, The minimal preprocessing pipelines for the Human Connectome Project. *NeuroImage* **80**, 105–124 (2013).

48. D. M. Barch, *et al.*, Function in the human connectome: task-fMRI and individual differences in behavior. *Neuroimage* **80**, 169–189 (2013).

49. M. Jenkinson, C. F. Beckmann, T. E. J. Behrens, M. W. Woolrich, S. M. Smith, FSL. *Neuroimage* **62**, 782–790 (2012).

50. B. Fischl, FreeSurfer. *Neuroimage* **62**, 774–781 (2012).

51. L. Griffanti, *et al.*, ICA-based artefact removal and accelerated fMRI acquisition for improved resting state network imaging. *Neuroimage* **95**, 232–247 (2014).

52. G. Salimi-Khorshidi, *et al.*, Automatic denoising of functional MRI data: combining independent component analysis and hierarchical fusion of classifiers. *Neuroimage* **90**, 449–468 (2014).

53. S. M. Smith, *et al.*, Functional connectomics from resting-state fMRI. *Trends Cogn. Sci. (Regul. Ed.)* **17**, 666–682 (2013).

54. M. F. Glasser, *et al.*, A multi-modal parcellation of human cerebral cortex. *Nature* **536**, 171–178 (2016).

55. E. C. Robinson, *et al.*, MSM: a new flexible framework for Multimodal Surface Matching. *Neuroimage* **100**, 414–426 (2014).

56. C. F. Beckmann, S. M. Smith, Probabilistic independent component analysis for functional magnetic resonance imaging. *IEEE Trans Med Imaging* **23**, 137–152 (2004).

57. A. Abrol, *et al.*, Replicability of time-varying connectivity patterns in large resting state fMRI samples. *Neuroimage* **163**, 160–176 (2017).

58. E. A. Allen, *et al.*, Tracking whole-brain connectivity dynamics in the resting state. *Cereb. Cortex* **24**, 663–676 (2014).

59. B. Rashid, *et al.*, A framework for linking resting-state chronnectome/genome features in schizophrenia: A pilot study. *Neuroimage* **184**, 843–854 (2019).

60. M. Rubinov, O. Sporns, Complex network measures of brain connectivity: Uses and interpretations. *NeuroImage* **52**, 1059–1069 (2010).

61. G. L. Colclough, *et al.*, The heritability of multi-modal connectivity in human brain activity. *Elife* **6** (2017).

62. A. I. Yashin, I. A. Iachine, Genetic analysis of durations: Correlated frailty model applied to survival of Danish twins. *Genetic Epidemiology* **12**, 529–538 (1995).

63. H. Akaike, Factor analysis and AIC. *Psychometrika* **52**, 317–332 (1987).

64. J. D. Power, K. A. Barnes, A. Z. Snyder, B. L. Schlaggar, S. E. Petersen, Spurious but systematic correlations in functional connectivity MRI networks arise from subject motion. *Neuroimage* **59**, 2142–2154 (2012).

65. H. Hotelling, Relations between two sets of variates. *Biometrika* **28**, 321–377 (1936).

Tables

Table 1. Variance-component model parameter estimates of the dynamic connectome features.

Phenotype	Model	h^2	(95% CI)	A	(95% CI)	C	(95% CI)	E	(95% CI)	-2LL	AIC	χ^2	Δdf	p
FO	ACE	.35	(.20, .50)	.35	(20, .50)	.00	(0.0, 0.0)	.65	(.50, .80)	-518.86	-504.86			
	AE	.35	(.19, .50)	.35	(.20, .50)			.65	(.50, .80)	-518.86	-506.86	2.4e-10	1	1.0
	CE					.27	(.14, .41)	.73	(.59, .86)	-516.57	-504.57	2.29	1	.13
TP	ACE	.41	(.27, .55)	.41	(.27,.55)	.00	(0.0, 0.0)	.59	(.45, .73)	-513.43	-499.43			
	AE	.41	(.27, .55)	.41	(.27, .55)			.59	(.45, .73)	-513.43	-501.43	8.1e-12	1	1.0
	CE					.33	(.21, .46)	.67	(.54, .79)	-510.89	-498.89	2.53	1	.11

All models were adjusted for age, sex, and head motion. A, Additive genetic effect; C, common environmental effect; E, Unique/non-shared environment effect; -2LL, twice the negative log-likelihood; AIC, Akaike's information criterion; df, degrees of freedom; χ^2, chi square, Δdf, change in degree of freedom between the full model and the nested model; *p*, χ^2 test in model fitting. The AE and CE models are nested within the ACE model. Each nested model is compared with the fully saturated model. The fitness of models was tested based on a change in AIC (for a change of df of 1, the statistically significant change in χ^2 is 3.84). h^2, the narrow-sense heritability estimated as $\sigma^2_A/(\sigma^2_A + \sigma^2_c + \sigma^2_E)$; CI: Confidence Interval (lower bound, upper bound).